Supplemental Table of Contents

Supplemental Methods

TERT DNA sequencing

TERT variant classification

Human TERT structural homology model

Figures

Figure S1. Summary of overall study analysis

Figure S2. Domain distribution of *TERT* variants in NHL cohort

Figure S3. Distribution of *TERT* rare variants by age younger or older than 40

Figure S4. Somatic mutations in patients with a *TERT* rare variant

Figure S5. Clonal markers and bone marrow blasts among patients with a *TERT* rare variant

Figure S6. *TERT* A1062T clinical characteristics and transplant outcomes

Figure S7. Transplant outcomes in patients with a *TERT* rare variant based on somatic mutation status

Figure S8. Transplant outcomes by *TERT* variant status and conditioning intensity

Figure S9. Univariate analyses of overall survival, NRM, and relapse by *TERT* variant status

Figure S10. Western blot summary of TERT rare variants

Figure S11. K562 *TERT* rare variant qPCR relative telomere length summary

Figure S12. Terminal restriction fragment analysis summary of *TERT* rare variants

Figure S13. Functional and structural characterization of the single NHL *TERT* rare variant

Tables

Table S1. Site-directed mutagenesis primers

Table S2. Extended *TERT* rare variant classification

Table S3. *TERT* common variant classification

Table S4. *TERT* rare variant clinical summary

Table S5. Extended patient characteristics by *TERT* variant status

Table S6. MDS mutations by *TERT* rare variant status

Table S7. HCT-CI components by *TERT* rare variant status

Table S8. Chromosome 7 abnormalities by *TERT* rare variant status

Table S9. Characteristics of patients with a *TERT* rare variant according to somatic mutation status.

Table S10. Multivariable models transplant outcomes

Table S11. Causes of death by *TERT* rare variant status

Table S12. *TERT* rare variant functional-structural summary

Supplemental Methods

***TERT* DNA sequencing**

Amplicon libraries were prepared with an Ion AmpliSeq Custom panel by using the Ampliseq Library Kit Plus (Thermo Fisher Scientific, USA) according to the manufacturer's protocol. These amplicons were partially digested before ligation of adapters and multiplex barcodes. Ligation products were purified with AMPure XP beads (Beckman Coulter, USA) and quantified using the Ion Library TaqMan Quantitation Kit (Thermo Fisher Scientific, USA). Libraries were normalized to 30 pM concentration and multiplexed in batches of no more than 96 samples for further processing. Templating and Ion 530 chip loading was performed on the Ion Chef (Thermo Fisher Scientific, USA) followed by sequencing on the Ion S5 (Thermo Fisher Scientific, USA) according to the manufacturer's instructions. Samples were sequenced to at least 150x average read depth. Raw reads were aligned with the TMAP alignment package and variants called using the VariantCaller plugin, both from the Torrent Suite software (Thermo Fisher Scientific, USA). Variant annotation was done using Annovar[47]. Intronic and synonymous variants and variants with less than 5 alternate reads or less than 10 total reads were excluded from the analysis.

***TERT* variant classification**

TERT variants were classified as "common" or "rare" using a maximum population allele frequency in gnomAD (v2.1.1) of 0.001 in any reference population. *TERT* common and rare variants were classified by consensus as benign (B), likely benign (LB), variant of unknown significance (VUS), likely pathogenic (LP) or pathogenic (P) according to ACMG/AMP[33] and Sherloc[34] guidelines through manual curation. *In silico* prediction models Combined Annotation-Dependent Depletion (CADD)[50] and ClinPred[51] were used

to estimate likelihood of pathogenicity of each variant. A CADD PHRED score of 20 or greater indicates a SNV is in the top 1% of deleterious variants across all possible SNVs in human genome reference (cadd.gs.washington.edu). A ClinPred score >0.5 is considered a prediction of pathogenicity for a given variant (sites.google.com/site/clinpred/).

hTERT structural homology model

The full human TERT TEN domain, RTD, and the template-primer complex were modeled using the *Tetrahymena thermophila* telomerase holoenzyme cryo-EM structure (PDB accession code: 6D6V). The human TERT RBD domain bound to TR was modeled using the crystal structure of *Takifugu rubripes* TERT RBD-TR CR4/5 complex (PDB accession code: 4LMO) as a template. The solved crystal structures of human TERT CTE (PDB accession code: 5UGW) and human TPP1-OB (PDB: 2I46) were used as such. The full model of human telomerase-TPP1-OB was assembled from these individual homology models by using the *Tetrahymena thermophila* telomerase holoenzyme cryo-EM reconstruction (PDB accession code: 6D6V) as a scaffold. The human TERT TEN, RT (and associated template-primer duplex), RBD (and associated CR4/5 RNA), and CTE were superimposed on their counterparts in the *Tetrahymena thermophila* telomerase holoenzyme reconstruction in Pymol using the “Align” command to assemble the human telomerase part of the homology model. Human TPP1-OB was superimposed on the p50 subunit of the *Tetrahymena thermophila* telomerase holoenzyme reconstruction to complete the human telomerase-TPP1 homology model. While TERT and TPP1 amino acids in the homology model correspond to sequences found in the human polypeptides, the original sequences and structures were retained for TR (*Tetrahymena thermophila* TR sequence for the template region and *Takifugu rubripes* TR sequence for the CR4/5 domain) and primer (*Tetrahymena thermophila* telomeric DNA primer sequence) regions in the homology model. No energy minimization or other refinement of the homology model was performed after assembly from individual components.

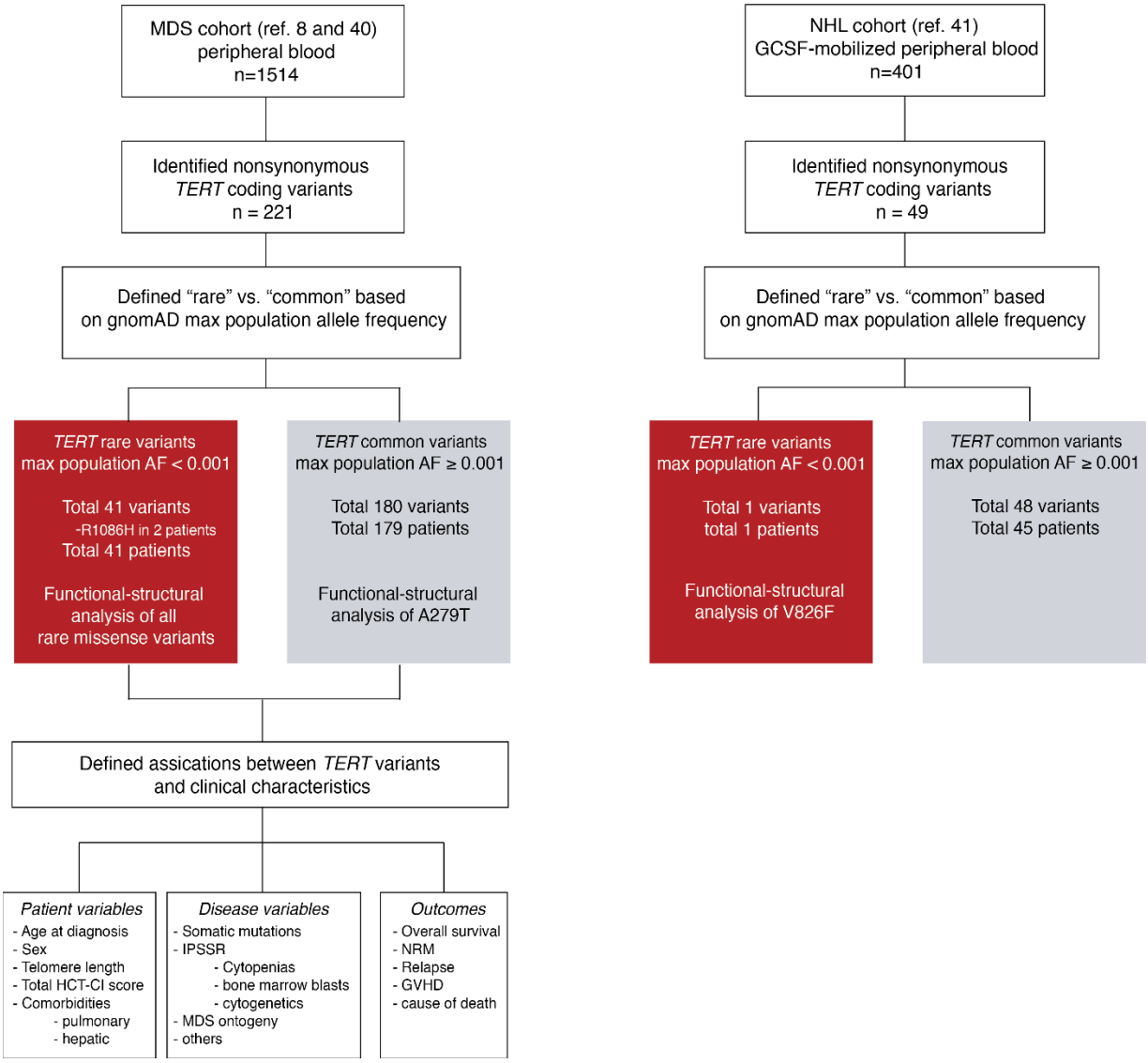

Supplementary Figure 1. Summary of overall study analysis. The *TERT* coding region was sequenced in the MDS and NHL cohorts. Nonsynonymous *TERT* coding variants were classified as either 'rare' or 'common' based on a gnomAD maximum population allele frequency (AF) cutoff of 0.001. The associations between the presence of *TERT* rare variants were analyzed with respect to clinical variables, disease variables, and transplant outcomes.

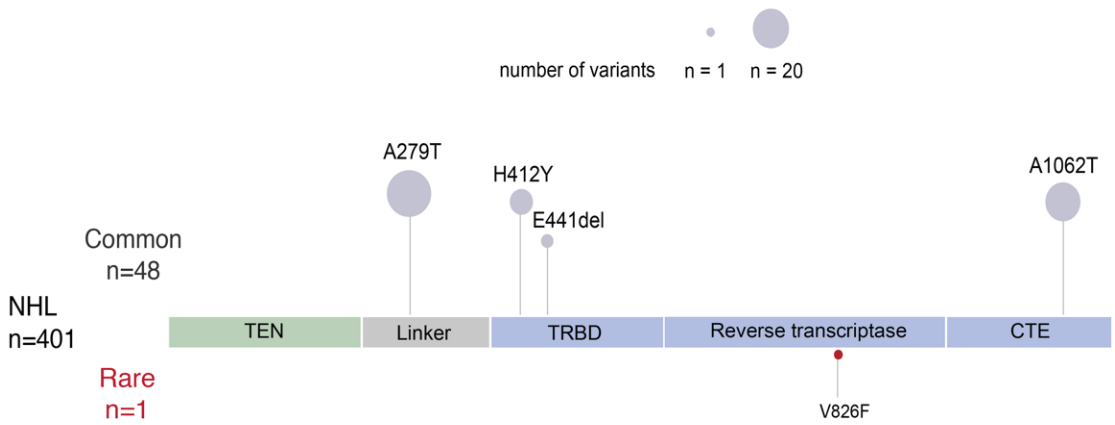

Supplemental Figure 2. Domain distribution of *TERT* variants within the NHL cohort. *TERT* common variants (n = 48) and the single rare variant (n =1) are located above and below the coding region, respectively. The size of each ball is proportional to the number of patients with that variant. The single *TERT* rare variant is colored in red and *TERT* common variants in gray.

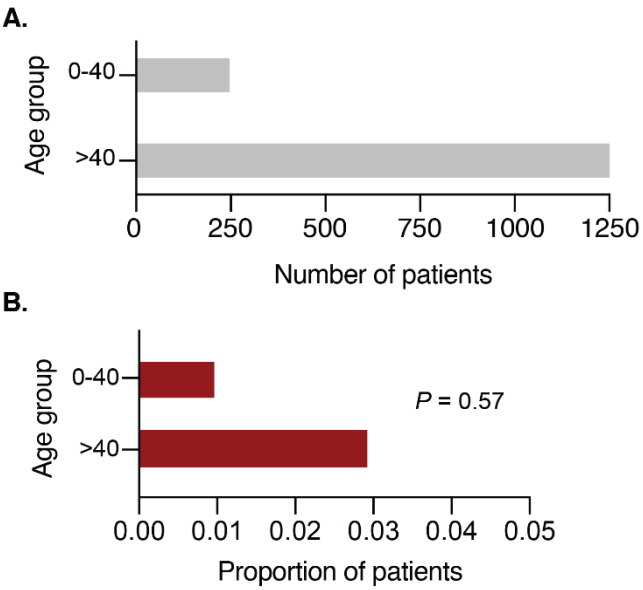

Supplemental Figure 3. Distribution of *TERT* rare variants by age younger or older than 40. Panel A shows the number of patients in the MDS cohort by age group (0-40 years and >40 years). Panel B shows the proportion of patients with a TERT rare variant by age group.

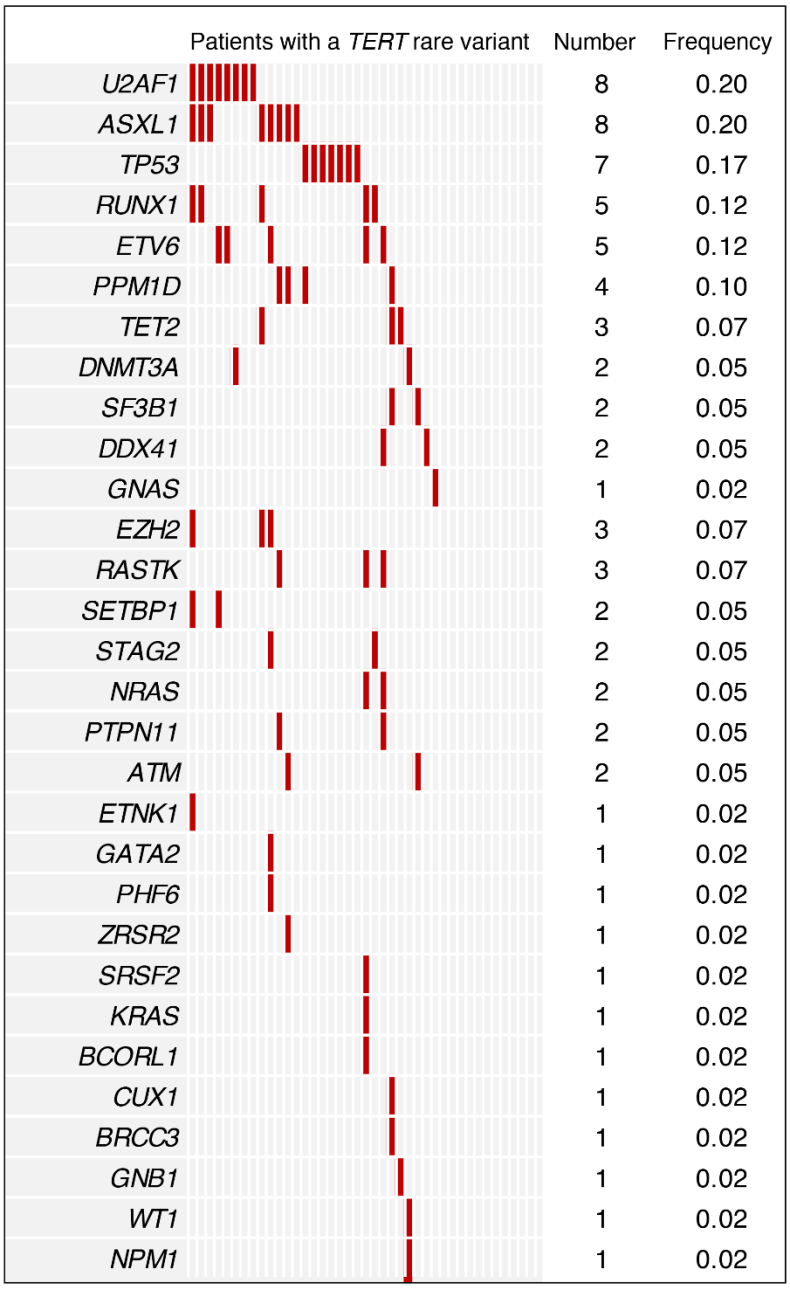

Supplemental Figure 4. Somatic mutations in patients with a *TERT* rare variant. Each column represents a patient with a *TERT* rare variant in the MDS cohort. Red boxes indicate the presence of a somatic mutation in the respective gene. Number and frequency of gene mutations are listed on the right of the panel.

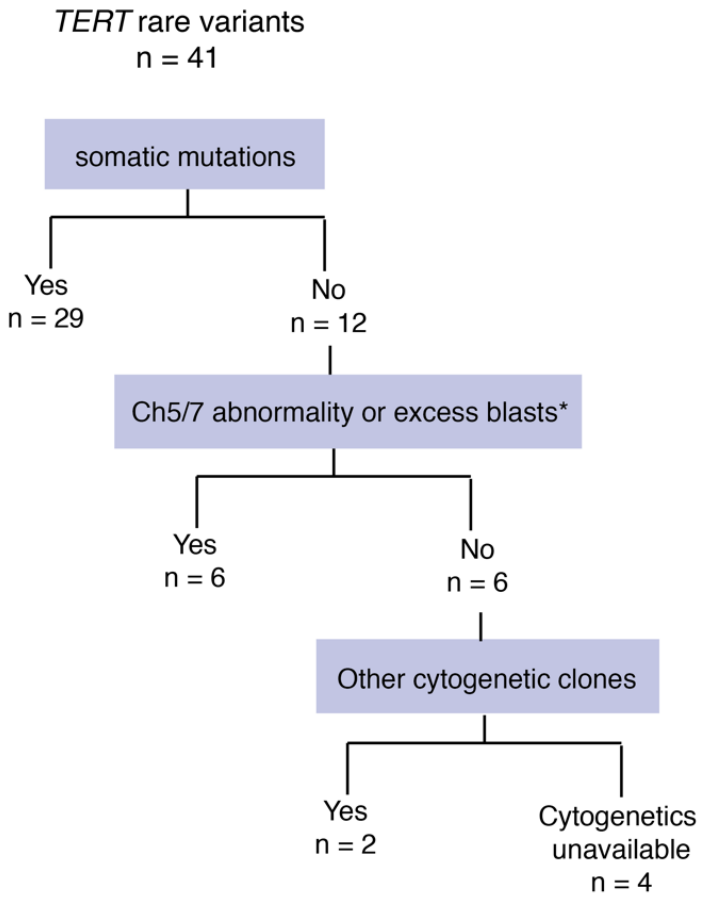

Supplemental Figure 5. Clonal markers and bone marrow blasts among patients with a *TERT* rare variant. Flow chart of patients with *TERT* rare variants based on presence or absence of myeloid somatic mutations, MDS-defining cytogenetic abnormalities, or other cytogenetic clones. Four patients did not have available cytogenetic data. (*) refers to -5/-5q, -7/7q, and/or bone marrow blasts ≥5%.

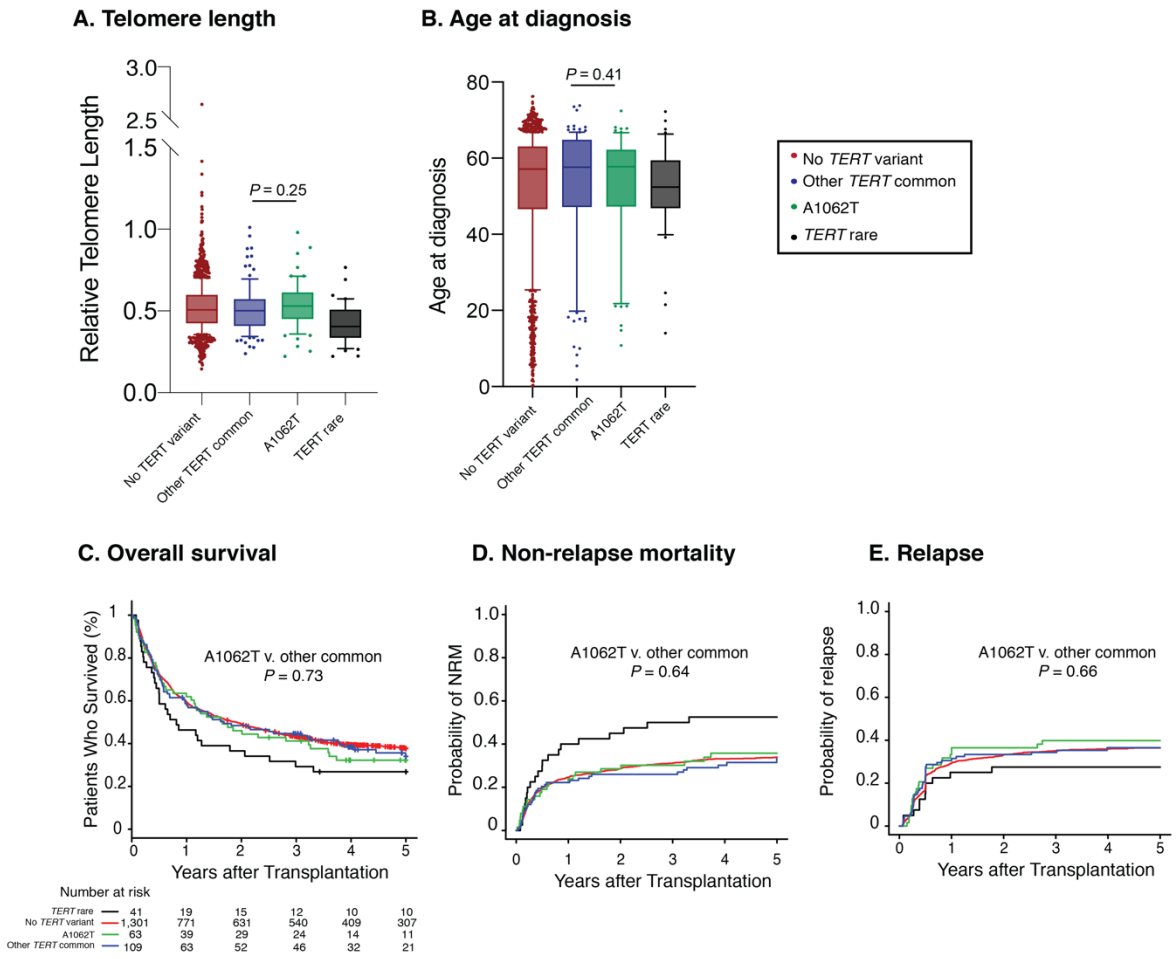

Supplemental Figure 6. *TERT* A1062T clinical characteristics and transplant outcomes. Panel A and B show relative telomere length and age at MDS diagnosis according to TERT variant status, respectively. Overall survival and the cumulative incidences of NRM and relapse are show in panels C-E according to *TERT* variant status: No *TERT* rare (red), A1062T (green), other *TERT* common (blue), and *TERT* rare (black).

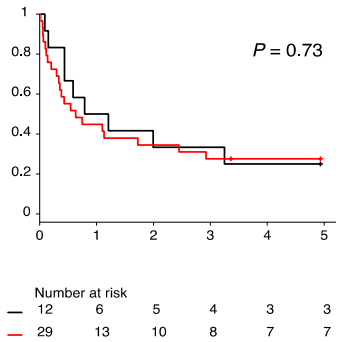

Supplemental Figure 7. Transplant outcomes in patients with a *TERT* rare variant based on somatic mutation status. Panels A, B, and C show the Kaplan-Meier curve of overall survival, the cumulative incidence of NRM, and the cumulative incidence of relapse for patients with a *TERT* rare variant, respectively. Patients with somatic mutations colored in red and patients without somatic mutations are labelled black.

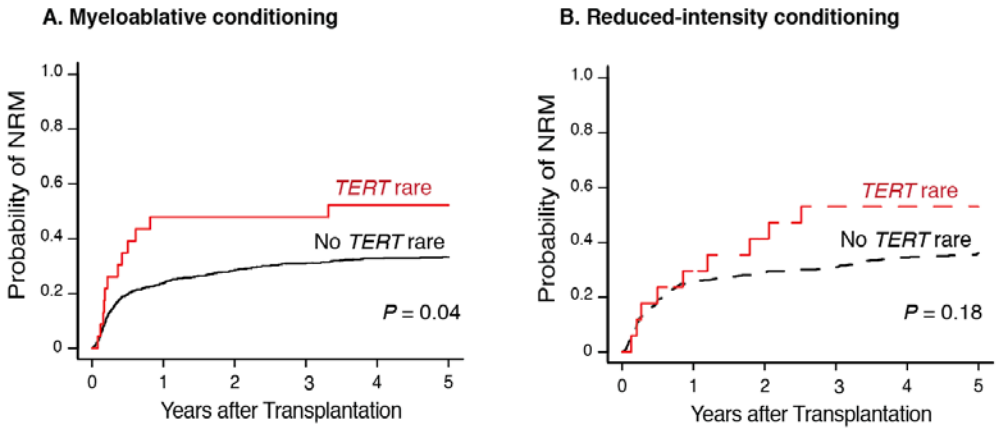

Supplemental Figure 8. Transplant outcomes by *TERT* rare variant status and conditioning intensity. Cumulative incidence of NRM in patients receiving myeloablative conditioning (A – solid lines) and reduced—intensity conditioning (B – dashed lines) according to *TERT* rare variant status (*TERT* rare in red and no *TERT* rare in black)

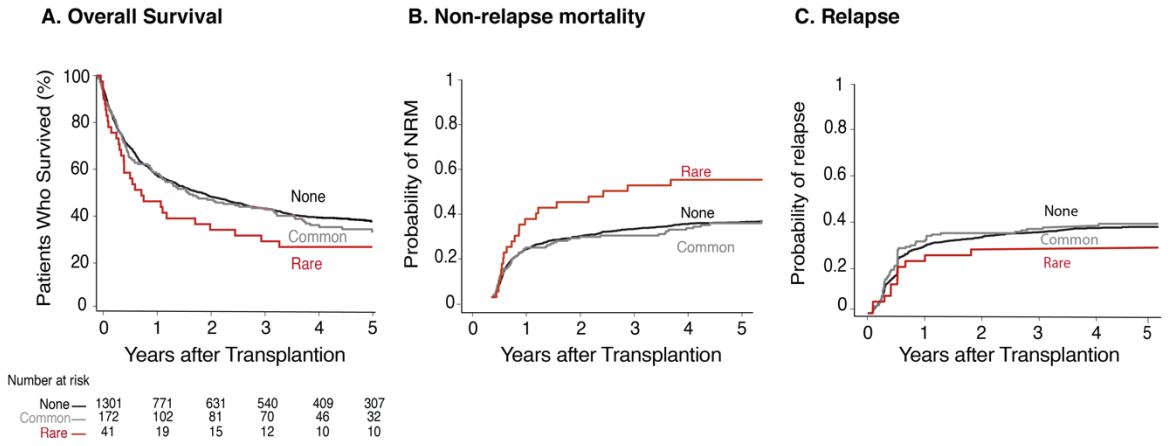

Supplemental Figure 9. Univariate analyses of overall survival, NRM, and relapse by *TERT* variant status. A) Kaplan-Meier curve of overall survival. B) Cumulative incidence curve for non-relapse mortality. C) Cumulative incidence curve for relapse. Patients with a *TERT* rare variants, *TERT* common variants, or no *TERT* variant are colored in red, gray, and black, respectively.

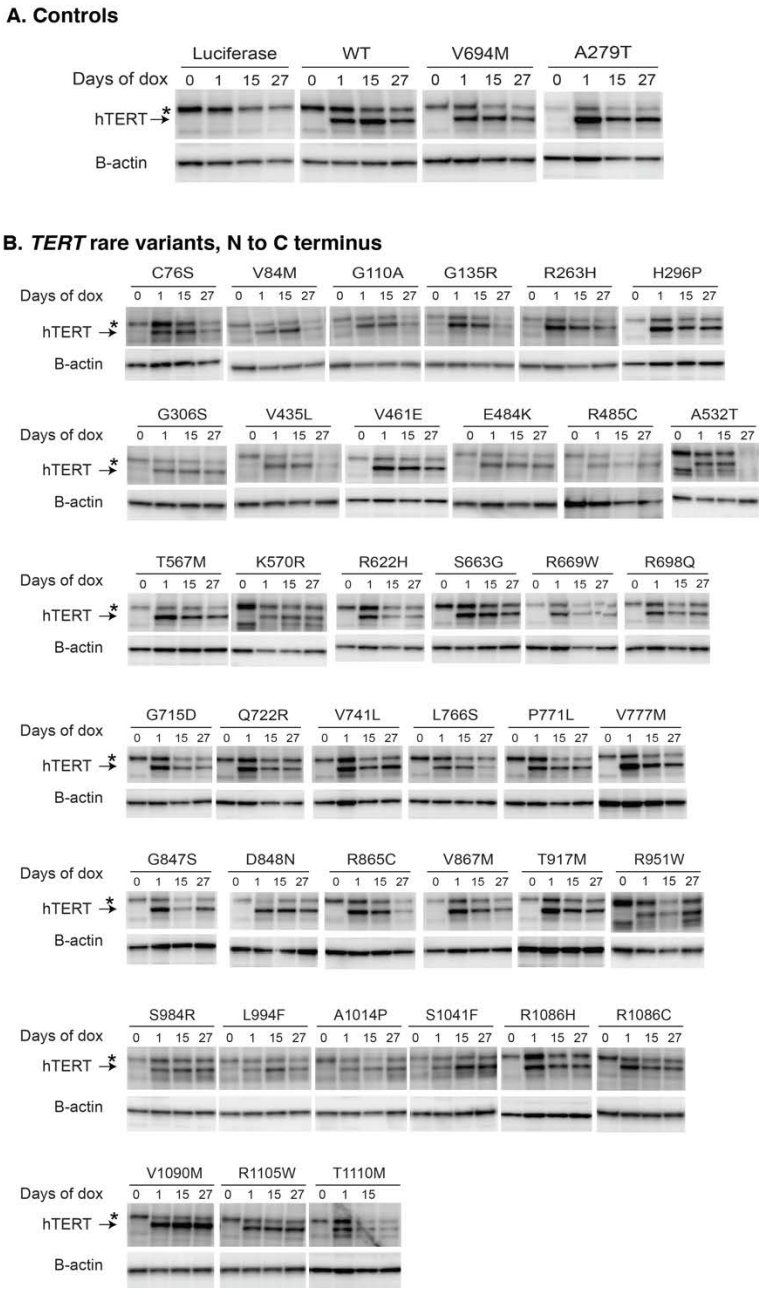

Supplemental Figure 10. Western blot summary of TERT rare variants. Induced expression of hTERT was measured at Day 0 prior to starting doxycycline and Day 1, 15, and 27 during the experiment. Arrow corresponds to the expected molecular weight of hTERT (~127 kDa) and asterisks corresponds to non-specific band seen in all conditions. A) Control conditions: luciferase, $TERT^{WT}$, $TERT^{V694M}$, and the common variant $TERT^{A279T}$. B) *TERT* rare variants from N to C terminus.

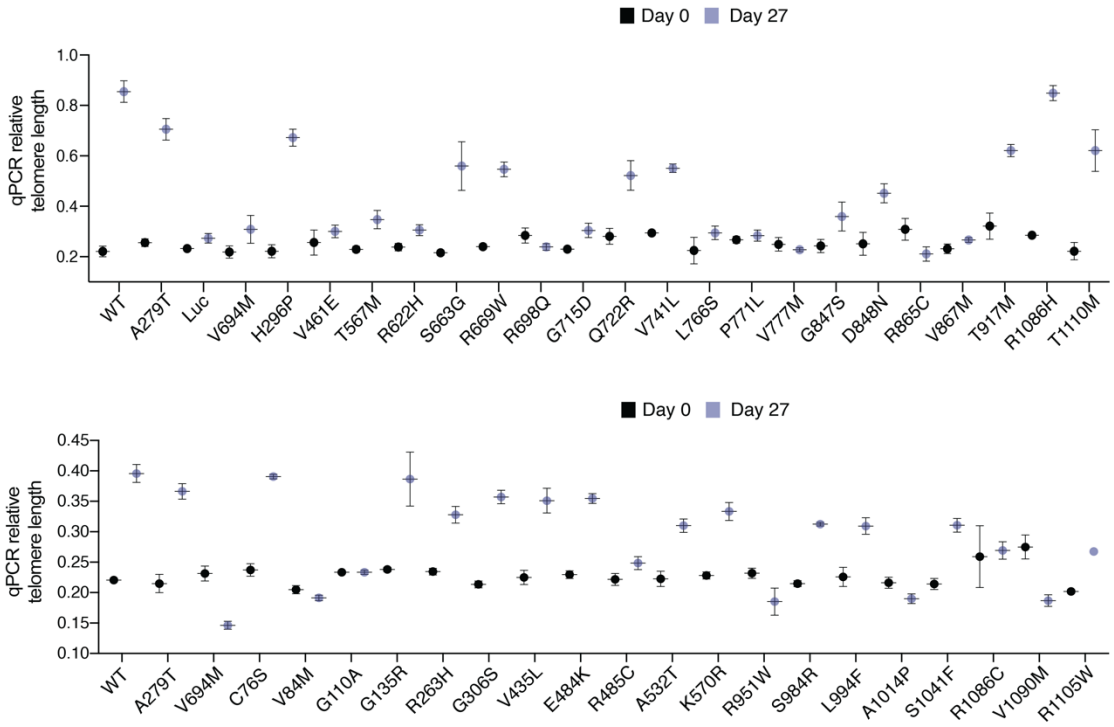

Supplemental Figure 11. K562 TERT rare variant qPCR relative telomere length summary. Graphs of relative telomere length measurements for each TERT rare variant at the beginning (Day 0 - black) and end (Day 27 - blue) of the experiment. Error bars correspond to standard deviation of triplicate values. qPCR measurements for all variants were performed in two batches.

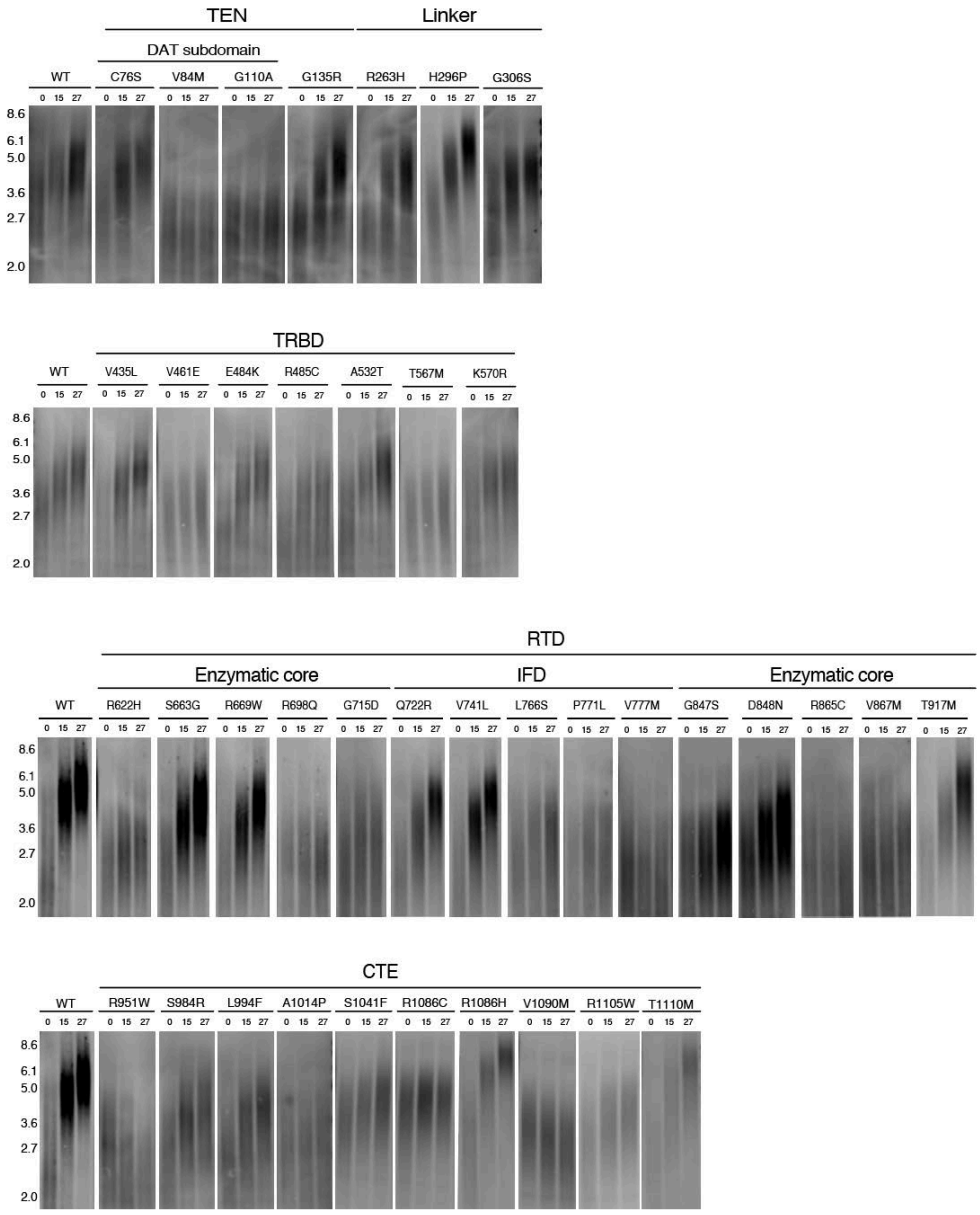

Supplemental Figure 12. Terminal restriction fragment analysis summary of TERT rare variants.

TRF images of 2ug digested genomic DNA extracted at Day 0, 15, and 27 for each TERT variant run on 1% agarose gel. Variants are arranged by structural domain and depict data from multiple gels.

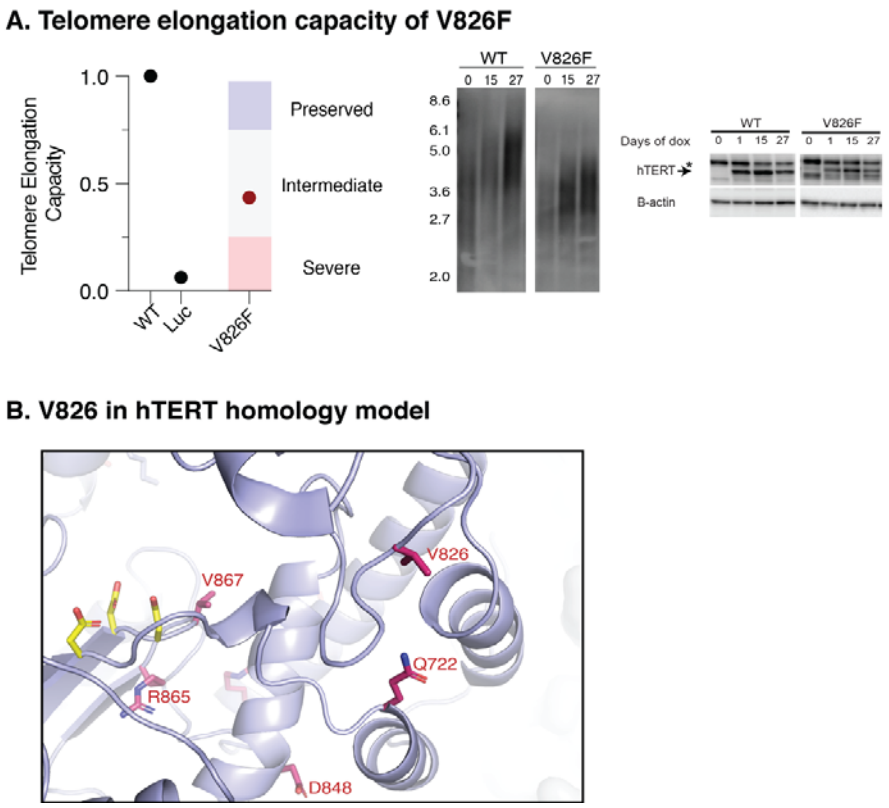

Supplemental Figure 13. Functional and structural characterization of the single NHL *TERT* rare variant V826F. Panel A shows telomere elongation capacity calculated using qPCR TL data and corresponding TRF and hTERT western blot; (*) indicates non-specific band and the arrow corresponds to hTERT. Panel B shows the position of V826 within the enzymatic core of the RTD.

Supplemental Table 1. Site-directed mutagenesis primers

TERT rare variant	Forward Primer	Reverse Primer
C76S	CAGGTGTCCTCCCTGAAGGAGCTGGTGG	GCGGAAGGAGGGGGCGGC
V84M	GGTGGCCCGAATGCTGCAGAG	AGCTCCTTCAGGCAGGACACC
G110A	GCCCGCGGGGCCCCCCCCGAG	CCCGTCCAGCAGCGCGAAGCCG
G135R	GCGGGGGAGCAGGGCGTGGGG	AGTGCGTCGGTCACCGTGTTGGG
R263H	GGCAGGACGCATGGACCGAGTG	CGGGTGGGCCCAGGACCC
A279T	TGCCAGACCCACCGAAGAAGC	GGTGACACCACACAGAAAC
H296P	CGCCACTCCCCCCCATCCGTG	CGTGCCAGAGAGCGCACC
G306S	GCACCACGCGAGCCCCCCATC	TGGCGGCCCACGGATGGG
V435L	CCAGGGCTCTCTGGCGGCCCC	GGCTTCTCCCGGGCACAG
V461E	CCCTGGCAGGAGTACGGCTTC	GCTGCTGTGCTGGCGGAG
E484K	CAGGCACAACAAACGCCGCTTCC	GAGCCCCAGAGGCCTGGG
R485C	GCACAACGAATGCCGCTTCCTC	CTGGAGCCCCAGAGGCCT
A532T	TGTTCCGGCCACAGAGCACCG	CAGCCAACCCCTGGGCTC
T567M	ACGGAGACCATGTTTCAAAAG	GACATAAAAGAAAGACCTGAG
K570R	ACGTTTCAAAGGAACAGGCTC	GGTCTCCGTGACATAAAAG
R622H	TCCAGACTCCACTTCATCCCCAAGCCTGAC	CGTCAGCAGGGCGGGCCT
S663G	GGCACTGTTCGGCGTGCTCAA	TTCACCCTCGAGGTGAGAC
R669W	CAACTACGAGTGGGCGCGGCG	AGCACGCTGAACAGTGCCTTC
V694M	GCGCACCTTCATGCTGCGTGT	CAGGCCCTGTGGATATCGTC
R698Q	CTGCGTGTGCAGGCCCAGGAC	CACGAAGGTGCGCCAGGC
G715D	GATGTGACGGACGCGTACGAC	CACCTTGACAAAGTACAGCTC
Q722R	ACCATCCCCCGGGACAGGCTC	GTCGTACGCGCCCGTCAC
V741L	CACGTACTGCCTGCGTCGGTA	TTCTGGGGTTTGATGATGC
L766S	GTCTCTACCTCGACAGACCTCC	GTGGCTCTTGAAGGCCTT
P771L	GACCTCCAGCTGTACATGCGA	TGTCAAGGTAGAGACGTGG
V777M	GCGACAGTTCATGGCTCACCT	ATGTACGGCTGGAGGTCT
G847S	CCTGTGCTACAGCGACATGGAG	CTGCAGAGCAGCGTGGAG
D848N	GTGCTACGGCAACATGGAGAACAAG	AGGCTGCAGAGCAGCGTG
R865C	GCTGCTCCTGTGTTTGGTGGATGATTTC	CCGTCCCGCCGAATCCCC
V867M	CCTGCGTTTGATGGATGATTTCTTGTTGGTGACACC	AGCAGCCCGTCCCGCCGA
T917M	CTGGGTGGCATGGCTTTTGTT	GGCCTCGTCTTCTACAGG
R951W	CAGCTATGCCTGGACCTCCAT	GAGTAGTCGCTCTGCACC
S984R	AGTGTCACAGGCTGTTTCTGGATTTG	TCAGCCGCAAGACCCCAA
L994F	GGTGAACAGCTTCCAGACGGT	TGCAAATCCAGAAACAGGC
A1014P	CAGGTTTCACCCATGTGTGCTGCAG 3	TACGCCTGCAGCAGGAGG
S1041F	GACACGGCCTTCCTCTGCTAC	AGAGATGACGCGCAGGAAAAATG
R1086C	GACTCGACACTGTGTCACCTA	AGCTTGAGCAGGAATGCT
R1086H	ACTCGACACCATGTCACCTAC	CAGCTTGAGCAGGAATGC
V1090M	TGTCACCTACATGCCACTCCT	CGGTGTCGAGTCAGCTTG
R1105W	GCAGCTGAGTTGGAAGCTCCC	GTCTGGGCTGTCCTGAGTG
T1110M	CTCCCGGGGATGACGCTGACT	CTTCCGACTCAGCTGCGTC

Supplemental Table 2. Extended *TERT* rare variant classification

Ch 5 genomic position	Ref	Alt	*TERT* rare variant	ACMG/AMP Criteria	Sherloc Criteria	ClinPred score	PMID Reference
1294774	C	G	p.C76S	PM2; BP4	EV01035	0.05921087	
1294751	C	T	p.V84M	PM2; PP3	EV01035	0.90967768	
1294672	C	G	p.G110A	PM2; PP3, PP5	EV01035, EV0061, EV0053	0.42297935	26024875
1294598	C	T	p.G135R	PM2	EV0161	0.02669442	
1294213	C	T	p.R263H	PM2; BP4	EV01035, EV0126	0.20593388	
1294114	T	G	p.H296P	PM2; BP4	EV0161, EV0126	0.05764545	
1294085	C	T	p.G306S	PM2; BP4	EV01035, EV0126	0.04076032	
1293698	C	G	p.V435L	PM1, PM2; BP4	EV01035, EV0172 EV0126	0.12568937	
1293619	A	T	p.V461E	PM1, PM2; PP3	EV01035, EV0172 EV0122	0.99402605	
1293551	C	T	p.E484K	PM1, PM2; BP4	EV01035, EV0172 EV0126	0.02799475	
1293548	G	A	p.R485C	PM1, PM2	EV0101, EV0172, EV0024	0.0912887	17460043
1282719	C	T	p.A532T	PM1, PM2; BP4	EV0101, EV0172, EV0126	0.05038688	
1282613	G	A	p.T567M	PM1, PM2; PP3	EV01035, EV0172, EV0053	0.71335232	23538340
1282604	T	C	p.K570R	PM1, PM2, PM5; PP3	EV01035, EV0172, EV0044	0.86071074	
1280455	T	C	c.1770-2A>G	PM2	EV01035, EV0172	n/a	
1280358	C	T	p.R622H	PM1, PM2; PP3	EV01035, EV0172, EV0122	0.9958812	25346280
1279549	T	C	p.S663G	PM1, PM2	EV01035, EV0172	0.14513995	
1279531	G	A	p.R669W	PM1, PM2; PP3	EV0101, EV0172, EV0122	0.94496411	
1279443	C	T	p.R698Q	PM1, PM2; PP3	EV01035, EV0172, EV0081	0.45770326	22664374
1278898	C	T	p.G715D	PM1, PM2; PP3	EV01035, EV0172	0.99102062	
1278877	T	C	p.Q722R	PM1, PM2; PP3	EV01035, EV0172	0.97397363	
1278821	C	A	p.V741L	PM1, PM2	EV0101, EV0172	0.07110612	
1272385	A	G	p.L766S	PM1, PM2; PP3	EV01035, EV0172	0.5904355	
1272370	G	A	p.P771L	PM1, PM2; PP3	EV01035, EV0172	0.99044496	
1272353	C	T	p.V777M	PM1, PM2, PM5, PP3	EV01035, EV0172	0.92925555	25741868
1268678	C	T	p.G847S	PM1, PM2; PP3	EV0101, EV0172	0.99762005	
1268675	C	T	p.D848N	PM1, PM2; PP3	EV0101, EV0172	0.9248184	
1266640	G	A	p.R865C	PM1, PM2; PP3, PP5	EV0101, EV0172, EV0024, EV0122	0.99269283	17460043
1266634	C	T	p.V867M	PM1, PM2; PP3	EV01035, EV0172, EV0024	0.82887769	20502709
1264612	G	A	p.T917M	PM1, PM2; PP3	EV0101, EV0172	0.27089664	
1260708	G	A	p.R951W	PM2; PP1, PP3	EV0101, EV0051, EV0024, EV0122	0.67566538	20502709; 27540018
1260607	G	C	p.S984R	PM2; BP4	EV0101	0.31716758	
1258765	G	A	p.L994F	PM2	EV0101	0.44978669	
1255519	C	G	p.A1014P	PM2; PP3	EV01035	0.98364198	
1255437	G	A	p.S1041F	PM2; PP3	EV01035	0.87835681	
1254522	G	A	p.R1086C	PM2	EV01035, EV0122	0.96164751	28099038
1254521	C	T	p.R1086H	PM2	EV0161	0.05256126	
1254510	C	T	p.V1090M	PM2; PP5	EV0161, EV0080, EV0024	0.03671261	15814878; 23901009
1253929	G	A	p.R1105W	PM2; PP3	EV01035, EV0221	0.73196268	
1253913	G	A	p.T1110M	PM2; PP6	EV0161, EV0221	0.04365337	17392301

Supplemental Table 3. *TERT* common variant classification

Ch 5 genomic position	Reference	Alternate	*TERT* common variant	Structural domain	gnomAD max popAF	ACMG/AMP classification	Sherloc classification	ClinVar Accession Number
1294429	C	G	p.S191T	TEN	0.003646	LB	LB	VCV000350804
1294397	C	T	p.A202T	TEN	0.00182	LB	LB	VCV000012729
1294166	C	T	p.A279T	TEN	0.1209	B	B	VCV000039125
1294163	C	T	p.E280K	TEN	0.00277	LB	LB	VCV000471904
1293767	G	A	p.H412Y	TRBD	0.0188	B	B	VCV000012730
1293677	0	-	p.E441del	TRBD	0.003621	LB	LB	VCV000212398
1293665	G	T	p.R446S	TRBD	0.002254	LB	LB	VCV000242216
1254594	C	T	p.A1062T	CTE	0.02149	B	B	VCV000039121

Supplemental Table 4. *TERT* rare variant clinical summary

Patient ID	RTL	Age at transplant	*TERT* rare variant	Variant alle fraction (VAF)
131-871-9	0.530985789	59.7	p.C76S	0.5517
632-160-1	0.338146726	52.6	p.V84M	0.500
167-534-0	0.38999983	68.0	p.G110A	0.3882
012-006-6	0.766510528	58.5	p.G135R	0.624
004-659-9	0.574438667	56.9	p.R263H	0.513
695-506-9	0.292339718	25.1	p.H296P	0.4486
193-453-1	0.475952599	72.9	p.G306S	0.4981
108-599-5	0.559849249	59.1	p.V435L	0.4764
006-488-1	0.257154532	49.4	p.V461E	0.526
684-474-3	0.412026455	63.3	p.E484K	0.4905
182-114-2	0.350501483	66.2	p.R485C	0.4228
202-087-6	0.557648152	45.9	p.A532T	0.4974
188-048-6	0.223210607	46.6	p.T567M	0.5269
112-386-1	0.516129796	60.6	p.K570R	0.4749
139-119-5	0.225024512	73.0	c.1770-2A>G	0.4609
199-354-5	0.405217397	52.9	p.R622H	0.422
672-577-7	0.401343382	52.8	p.S663G	0.5024
680-768-2	0.440760004	49.7	p.R669W	0.5181
622-265-0	0.394371706	44.2	p.R698Q	0.5228
675-834-9	0.329298568	45.4	p.G715D	0.3652
138-295-4	0.57269467	55.7	p.Q722R	0.4072
646-745-3	0.411590539	70.6	p.V741L	0.4719
631-993-6	0.32504369	48.2	p.L766S	0.4414
116-369-3	0.335353357	47.1	p.P771L	0.5012
658-186-5	0.343358458	57.0	p.V777M	0.5204
126-140-6	0.291944859	52.3	p.G847S	0.4721
169-536-3	0.336384474	50.9	p.D848N	0.4718
137-528-9	0.317172711	48.4	p.R865C	0.4533
618-645-9	0.462689547	60.3	p.V867M	0.4801
653-872-5	0.418968207	62.0	p.T917M	0.5008
648-041-5	0.356232164	53.0	p.R951W	0.465
694-861-9	0.692395209	49.3	p.S984R	0.4878
637-301-6	0.545545414	39.7	p.L994F	0.5012
618-695-4	0.400868653	47.6	p.A1014P	0.4567
001-142-9	0.595007843	48.4	p.S1041F	0.4733
126-937-5	0.42325787	53.4	p.R1086C	0.4618
216-744-6	0.450950753	67.1	p.R1086H	0.3925
223-987-2	0.366835906	14.1	p.R1086H	0.4264
141-314-8	0.501318668	66.9	p.V1090M	0.4502
155-275-4	0.500527712	59.1	p.R1105W	0.5865
671-880-6	0.265103336	22.2	p.T1110M	0.4573

Supplemental Table 5. Extended patient characteristics by *TERT* variant status

	TERT variant		
	None	Common	Rare
	n = 1301	n = 172	n = 41
Patient-related variables			
Age at transplantation, median (range), years	59 (0 - 77)	59 (5 - 75)	52 (14 - 72)
Female sex, n (%)	519 (40)	72 (42)	11 (27)
Karnofsky performance status score < 90, n (%)	349 (27)	54 (31)	16 (39)
Hematopoietic cell transplant comorbidity index (HCT-CI)			
0	225 (24)	30 (25)	3 (11)
1-2	225 (24)	22 (19)	8 (29)
3	469 (51)	66 (56)	17 (61)
Missing	382	54	13
Disease-related variables			
Hemoglobin, median (interquartile range), g/dL	9.4 (8.1-11.2)	9.2 (8.0-11.0)	9.9 (8.6-11.1)
Platelet count, median (interquartile range), x 10^9/L	73 (30-148)	68 (23-140)	72 (37-115)
Absolute neutrophil count, median (interquartile range), x 10^9/L	1.1 (0.5-2.3)	1.4 (0.5-2.3)	1.3 (0.5-2.6)
Bone marrow blasts at transplant, median (interquartile range), %	3 (1-6)	2 (1-7)	1 (0-5)
IPSS-R cytogenetic risk group, n (%)			
Very good	8 (1)	-	1 (3)
Good	461 (45)	66 (48)	15 (43)
Intermediate	216 (21)	28 (20)	9 (26)
Poor	226 (22)	34 (25)	5 (14)
Very poor	107 (11)	10 (7)	5 (14)
Unknown	283	34	6
IPSS-R group, n (%)			
Very low	101 (10)	14 (11)	4 (13)
Low	249 (25)	27 (21)	11 (37)
Intermediate	285 (29)	49 (38)	6 (20)
High	196 (20)	21 (16)	6 (20)
Very high	149 (15)	19 (15)	3 (10)
Missing	321	42	11
Prior MDS-directed therapy, n (%)	763 (59)	98 (57)	24 (59)
Therapy-related MDS, n (%)	272 (21)	33 (19)	6 (15)
Monosomal karyotype, n (%)	180 (14)	25 (15)	5 (12)
Transplantation-related variables			
Conditioning regimen, n (%)			
Myeloablative	681 (52)	84 (49)	24 (59)
Reduced intensity	491 (38)	74 (43)	17 (41)
Nonmyeloablative	116 (9)	14 (8)	-
Missing	13	-	-
Donor type, n (%)			
Matched, Related	157 (12)	19 (11)	5 (12)
Matched, Unrelated	730 (56)	107 (62)	26 (63)
Mismatched	256 (20)	33 (19)	7 (17)
Cord Blood	158 (12)	13 (8)	3 (7)
Graft type, n (%)			
Bone marrow	189 (15)	26 (15)	6 (15)
Peripheral blood stem cells	950 (73)	132 (77)	32 (78)
Cord Blood	152 (12)	13 (8)	3 (7)
Other	10 (1)	1 (1)	-
Donor age			
Under 35	790 (61)	110 (64)	28 (70)
35 or older	495 (39)	61 (36)	12 (30)
Missing	16	1	1
Female donor, n (%)	396 (32)	45 (27)	13 (35)
In vivo T cell depletion, n (%)	521 (40)	71 (41)	13 (32)

GVHD prophylaxis, n (%)			
Tacrolimus-based	963 (74)	137 (80)	34 (83)
CSA-based	210 (16)	26 (15)	6 (15)
Other	39 (3)	2 (1)	1 (2)
CD34 selection	31 (2)	1 (1)	-
Ex vivo T-cell depletion	18 (1)	3 (2)	-
Cyclophosphamide-based	18 (1)	1 (1)	-
None reported	22 (2)	2 (1)	-
Year of transplantation			
≤2007	252 (19)	39 (23)	9 (22)
>2007	1,049 (81)	133 (77)	32 (78)

Unless otherwise stated, peripheral blood counts and bone marrow blast counts at time of transplantation
(-) indicates data not available

Supplemental Table 6. MDS mutations by *TERT* rare variant status

Gene	No *TERT* rare n = 1473 (%)	*TERT* rare n = 41 (%)	*P*
TP53	282 (19)	7 (17)	0.84
ASXL1	289 (20)	8 (20)	> 0.99
TET2	181 (12)	3 (7)	0.47
DNMT3A	225 (15)	2 (5)	0.08
RUNX1	169 (11)	5 (12)	0.81
RAS pathway	190 (13)	3 (7)	0.47
SF3B1	145 (10)	2 (5)	0.42
U2AF1	119 (8)	8 (20)	0.02
PPM1D	84 (6)	4 (10)	0.29
STAG2	94 (6)	2 (5)	> 0.99
SETBP1	88 (6)	2 (5)	> 0.99
SRSF2	95 (6)	1 (2)	0.51
NRAS	66 (4)	2 (5)	0.71
ETV6	57 (4)	5 (12)	0.02
PTPN11	54 (4)	2 (5)	0.66
GATA2	53 (4)	1 (2)	> 0.99
EZH2	54 (4)	3 (7)	0.20
PHF6	49 (3)	1 (2)	> 0.99
WT1	30 (2)	1 (2)	0.58
CUX1	29 (2)	1 (2)	0.56
ZRSR2	32 (2)	1 (2)	0.60
KRAS	28 (2)	1 (2)	0.55
NPM1	24 (2)	1 (2)	0.50
ETNK1	18 (1)	1 (2)	0.41
ATM	15 (1)	2 (5)	0.08
BRCC3	15 (1)	1 (2)	0.36
BCORL1	11 (1)	1 (2)	0.28
GNB1	10 (1)	1 (2)	0.26
GNAS	7 (0)	1 (2)	0.20
DDX41	67 (5)	2 (5)	0.71
None	306 (21)	12 (29)	0.24

P values calculated using Fisher's exact test.

Supplemental Table 7. HCT-CI components by *TERT* rare variant status

	Total n = 1514	No TERT rare n = 1473	*TERT rare* n = 41
Infection, n (%)			
No	1,142 (75)	1,111 (75)	31 (76)
Yes	69 (5)	68 (5)	1 (2)
Missing	303 (20)	294 (20)	9 (22)
Pulmonary, n (%)			
No	738 (49)	722 (49)	16 (39)
Moderate	292 (19)	282 (19)	10 (24)
Severe	179 (12)	173 (12)	6 (15)
Missing	305 (20)	296 (20)	9 (22)
Hepatic, n (%)			
No	1,121 (74)	1,092 (74)	29 (71)
Mild	71 (5)	68 (5)	3 (7)
Moderate/severe	18 (1)	18 (1)	-
Missing	304 (20)	295 (20)	9 (22)
Prior solid tumor, n (%)			
No	1,012 (67)	983 (67)	29 (71)
Yes	198 (13)	195 (13)	3 (7)
Missing	304 (20)	295 (20)	9 (22)
Arrhythmia, n (%)			
No	1,152 (76)	1,121 (76)	31 (76)
Yes	55 (4)	54 (4)	1 (2)
Missing	307 (20)	298 (20)	9 (22)
Cardiac, n (%)			
No	1,035 (68)	1,008 (68)	27 (66)
Yes	174 (11)	169 (11)	5 (12)
Missing	305 (20)	296 (20)	9 (22)
Diabetes, n (%)			
No	1,055 (70)	1,028 (70)	27 (66)
Yes	154 (10)	149 (10)	5 (12)
Missing	305 (20)	296 (20)	9 (22)
Renal, n (%)			
No	1,201 (79)	1,169 (79)	32 (78)
Yes	10 (1)	10 (1)	-
Missing	303 (20)	294 (20)	9 (22)
Inflammatory Bowel Disease, n (%)			
No	1,196 (79)	1,164 (79)	32 (78)

Yes	15 (1)	15 (1)	-
Missing	303 (20)	294 (20)	9 (22)
Psychiatric, n (%)			
No	994 (66)	971 (66)	23 (56)
Yes	215 (14)	206 (14)	9 (22)
Missing	305 (20)	296 (20)	9 (22)
Obesity, n (%)			
No	1,102 (73)	1,078 (73)	24 (59)
Yes	108 (7)	100 (7)	8 (20)
Missing	304 (20)	295 (20)	9 (22)
Cerebrovascular, n (%)			
No	1,182 (78)	1,150 (78)	32 (78)
Yes	25 (2)	25 (2)	-
Missing	307 (20)	298 (20)	9 (22)
Rheumatologic, n (%)			
No	1,175 (78)	1,145 (78)	30 (73)
Yes	35 (2)	33 (2)	2 (5)
Missing	304 (20)	295 (20)	9 (22)
Peptic Ulcer, n (%)			
No	1,190 (79)	1,161 (79)	29 (71)
Yes	20 (1)	17 (1)	3 (7)
Missing	304 (20)	295 (20)	9 (22)
Heart valve disease, n (%)			
No	1,184 (78)	1,153 (78)	31 (76)
Yes	25 (2)	24 (2)	1 (2)
Missing	305 (20)	296 (20)	9 (22)

Supplemental Table 8. Chromosome 7 abnormalities by *TERT* rare variant status

	Total (n = 1514)	No *TERT* rare (n = 1473)	*TERT* rare (n = 41)	*P*
-7/del7q, n (%)				
Present	293 (19)	285 (19)	8 (20)	*> 0.99‡*
Absent	334 (22)	325 (22)	9 (22)	
Missing	*887 (59)*	*863 (59)*	*24 (59)*	

‡Fisher's exact test

Supplemental Table 9. Characteristics of patients with a *TERT* rare variant according to somatic mutation status.

Patient	Age at diagnosis	Blast % at diagnosis	Somatic mutations	Prior aplastic anemia	IPSSR	Cytogenetic risk group	Ch5/7 abnormality
004-659-9	25.1	-	No	No	-	-	-
675-834-9	45.4	-	No	No	Int-2	Poor	yes
631-993-6	48.2	0	No	Yes	-	-	-
137-528-9	48.4	1	No	No	Int-2	Intermediate	Yes
001-142-9	48.4	-	No	No	-	-	-
694-861-9	49.3	16	No	No	Int-1	Intermediate	No
680-768-2	49.67	0	No	No	Int-2	Poor	Yes
138-295-4	55.7	16	No	No	Int-1	Poor	Yes
193-453-1	56.9	0	No	No	Int-2	Intermediate	Yes
653-872-5	62	5	No	No	-	Intermediate	-
182-114-2	66.2	0	No	No	Int-1	Good	-
139-119-5	72.9	1	No	No	Int-1	Good	No
223-987-2	14	-	Yes	No	-	Unknown	-
671-880-6	21.5	5	Yes	No	-	Poor	No
637-301-6	39.2	-	Yes	No	-	Unknown	-
622-265-0	42.4	1	Yes	No	Low	Good	-
202-087-6	45.4	2	Yes	No	Int-1	Good	-
188-048-6	43.9	1	Yes	No	Int-1	Good	-
116-369-3	46.7	8	Yes	No	Int-1	Good	-
618-695-4	47	-	Yes	No	Int-2	Intermediate	Yes
006-488-1	47.5	0	Yes	No	Int-2	Poor	Yes
169-536-3	45.4	9	Yes	No	Int-2	Good	No
126-140-6	51.9	2	Yes	No	Int-1	Good	No
632-160-1	52	14	Yes	No	Low	Good	-
672-577-7	52.4	10	Yes	No	Int-1	Good	-
199-354-5	52.4	5	Yes	No	Int-1	Very good	No
648-041-5	52.5	4	Yes	No	-	Very poor	Yes
126-937-5	53.2	7	Yes	No	Int-2	Very poor	Yes
695-506-9	54.6	10	Yes	No	-	Good	-
658-186-5	53.5	4	Yes	No	Int-1	Intermediate	No
012-006-6	57.8	-	Yes	No	-	Unknown	-
155-275-4	58.7	1	Yes	No	Low	Good	No
108-599-5	58.7	8	Yes	No	Int-2	Very poor	Yes
131-871-9	58.8	2	Yes	No	Int-1	Intermediate	No
618-645-9	60	12	Yes	No	Int-2	Very poor	Yes
112-386-1	60.1	12	Yes	No	Int-1	Very poor	No
684-474-3	62.4	-	Yes	No	Int-1	Intermediate	No
141-314-8	61.5	-	Yes	No	-	Good	-
216-744-6	66.7	-	Yes	No	Int-1	Good	-
167-534-0	67.6	9	Yes	No	High	Intermediate	Yes
646-745-3	69.8	0	Yes	No	Low	Good	-

(-) indicates data not available

Supplementary Table 10. Multivariable models of transplant outcomes

		Cox regression: overall survival		Competing risks regression: NRM		Competing risks regression: relapse	
	No. of patients	HR (95% CI)	p	HR (95% CI)	p	HR (95% CI)	p
***TERT* rare variant status**							
No rare variant (reference)	1473						
Rare variant	41	1.50 (1.04, 2.17)	0.03	1.75 (1.13, 2.71)	0.01	0.78 (0.42, 1.46)	0.44
***TP53* status**							
No mutation (reference)	1225						
Mutation	289	1.74 (1.49, 2.04)	< 0.001	1.03 (0.82, 1.31)	0.80	1.85 (1.51, 2.28)	< 0.001
IPSS-R Risk Category							
Other (reference)	1343						
Very high	171	1.46 (1.20, 1.78)	< 0.001	1.04 (0.78, 1.38)	0.81	1.41 (1.07, 1.85)	0.01
Donor group							
Matched, Related (reference)	181						
Matched, Unrelated	863	1.07 (0.71, 1.62)	0.73	1.16 (0.63, 2.15)	0.63	1.12 (0.71, 1.77)	0.63
Mismatched	296	1.48 (0.97, 2.25)	0.07	1.69 (0.90, 3.15)	0.10	0.95 (0.59, 1.53)	0.83
Cord Blood	174	1.91 (1.20, 3.03)	0.006	2.19 (1.10, 4.35)	0.03	0.96 (0.56, 1.64)	0.89
RAS-tyrosine kinase pathway mutation							
No mutation (reference)	1321						
Mutation	193	1.35 (1.12, 1.63)	0.002	1.02 (0.77, 1.34)	0.92	1.32 (1.02, 1.71)	0.04
Donor age							
< 35 years old (reference)	928						
35 years or older	568	1.22 (1.05, 1.42)	0.009	1.12 (0.92, 1.37)	0.24	1.00 (0.82, 1.22)	0.99
Missing	18	0.95 (0.50, 1.79)	0.87	0.59 (0.19, 1.85)	0.37	1.06 (0.58, 1.95)	0.86
Recipient age							
10-year increase	1514	1.23 (1.16, 1.30)	< 0.001	1.23 (1.14, 1.33)	< 0.001	0.98 (0.91, 1.04)	0.48
Year of transplant							
2005-2007 (reference)	300						
2008-2014	1214	0.77 (0.49, 1.19)	0.24	0.48 (0.26, 0.90)	0.02	1.86 (1.10, 3.14)	0.02
Karnofsky Performance Score							
90-100 (reference)	817						
10-80	419	1.27 (1.10, 1.48)	0.002	1.23 (1.02, 1.53)	0.03	0.99 (0.80, 1.22)	0.94
Missing	278	1.05 (0.87, 1.27)	0.59	0.95 (0.73, 1.24)	0.72	1.14 (0.90, 1.45)	0.27
HCT-CI							
0 (reference)	258						
1-2	255	1.29 (1.01, 1.65)	0.04	1.15 (0.83, 1.58)	0.40	1.20 (0.88, 1.63)	0.25
3 or above	552	1.47 (1.19, 1.83)	< 0.001	1.32 (0.99, 1.76)	0.06	1.07 (0.81, 1.40)	0.64
Missing	449	1.35 (0.86, 2.11)	0.19	0.78 (0.41, 1.47)	0.44	1.86 (1.12, 3.07)	0.02
Conditioning intensity							
Myeloablative (reference)	789						
Reduced intensity	582	0.90 (0.77, 1.04)	0.15	0.82 (0.67, 1.00)	0.05	1.29 (1.05, 1.58)	0.02
Nonmyeloablative	130	1.04 (0.81, 1.33)	0.78	0.60 (0.41, 0.90)	0.01	2.19 (1.60, 3.01)	< 0.001
Missing	13	0.99 (0.44, 2.24)	0.98	0.90 (0.28, 2.89)	0.85	2.49 (1.49, 4.16)	< 0.001

Supplemental Table 11. Causes of death by *TERT* rare variant status

	TERT rare variant	
	Present	Absent
	n = 28	n = 902
Cause of death, n (%)		
GVHD	0 (0)	146 (16)
Non-infectious pulmonary disease	6 (21)	69 (8)
Other malignancy	2 (7)	19 (2)
Organ failure	3 (11)	67 (7)
Primary disease	9 (32)	347 (38)
Infection	5 (18)	139 (15)
Other	3 (11)	115 (13)

Supplemental Table 12. *TERT* rare variant functional and structural analysis summary

TERT rare variant	Telomere elongation capacity		hTERT homology model structural comments
p.C76S	preserved	0.88	Surface residue within DAT subdomain implicated in TPP1 binding; Ser results in mild change but decreased hydrophobicity; predicted likely tolerated.
p.V84M	severe	<0.0	Core residue in DAT subdomain implicated in TPP1 binding; Met substitution increases bulk but preserves hydrophobicity; predicted likely tolerated
p.G110A	severe	0.00	Not modeled but within DAT subdomain implicated in TPP1 binding; predicted pobably tolerated.
p.G135R	preserved	0.84	Located distal to DAT subdomain; Arg predicted to disrupt helix orientation and impair TPP1 binding; predicted likely pathogenic.
p.R263H	intermediate	0.53	Not modeled
p.H296P	intermediate	0.71	Not modeled
p.G306S	preserved	0.82	Not modeled
p.V435L	intermediate	0.72	Not modeled but likely in unstructured loop at a distance from RNA; predicted tolerated.
p.V461E	severe	0.07	In hydrophobic core; Glu likely disrupts folding; predicted pathogenic.
p.E484K	intermediate	0.71	Acidic residue in basic patch close to RNA; Lys could destabilize the basic helix; Predicted likely pathogenic
p.R485C	severe	0.15	On basic surface close to RNA binding groove; Cys results in loss of positive charge; predicted pathogenic
p.A532T	intermediate	0.50	On a helix that binds CR4/CR5 domain; Thr reduces hydrophobicity; predicted likely tolerated.
p.T567M	severe	0.18	On a hydrophilic loop close to the RNA-DNA duplex; Met increases bulk; predicted likely pathogenic
p.K570R	intermediate	0.60	On a hydrophilic loop close to RNA-DNA duplex; Arg maintains positive charge; predicted likely tolerated.
c.1770-2A>G	n/a	n/a	Not modeled
p.R622H	severe	0.07	Close to the template phosphodiester backbone; His likely disrupts this interaction; predicted pathogenic
p.S663G	intermediate	0.53	Surface residue facing IFD; Gly unlikely to produce significant change in structure; predicted likely tolerated
p.R669W	intermediate	0.48	Residue inserts between two helices; Trp could be accommodated; predicted likely tolerated
p.R698Q	severe	<0.0	Surface residue that forms H-bond to a beta-turn. Gln would allow H-bond; predicted likely tolerated.
p.G715D	severe	0.12	Active site residue; Asp would repel DNA-RNA duplex; predicted pathogenic
p.Q722R	intermediate	0.38	On a IFD bracing helix; Arg adds positive charge; predicted likely pathogenic.
p.V741L	intermediate	0.41	Hydrophobic IFD reside; Leu is minimal change; predicted tolerated.
p.L766S	severe	0.12	Hydrophobic IFD residue facing enzymatic core. Ser reduces hydrophobicity; predicted likely tolerated.
p.P771L	severe	0.03	Surface residue at TEN-IFD junction that could be involved in TPP1 interactions; retained hydrophobicity; predicted likely pathogenic.
p.V777M	severe	<0.0	Residue of IFD helix contacting TEN and TPP1; Met increases bulk; predicted pathogenic.
p.G847S	severe	0.18	Residue forms a kink in a long helix; Ser could disrupt conformation; predicted pathogenic.
p.D848N	intermediate	0.32	Residue faces IFD bracing helices; Asn may disrupt salt bridge with R724; predicted likely pathogenic.
p.R865C	severe	<0.0	Active side residue; Cys leads to loss of salt bridge with E850; predicted pathogenic.
p.V867M	severe	0.06	Residue in close proximity to DNA; Met increases bulk; predicted likely pathogenic
p.T917M	intermediate	0.48	Surface residue away from any interface; Met increases hydrophobicity; predicted likely tolerated.
p.R951W	severe	<0.0	Not modeled or conserved; predicted likely tolerated.
p.S984R	intermediate	0.56	Surface residue away from any interface; predicted tolerated
p.L994F	intermediate	0.48	Hydrophobic region and Phe will increase bulk; predicted likely tolerated.

p.A1014P	severe	<0.0	Strongly conserved and likely helix-breaking; predicted pathogenic.
p.S1041F	intermediate	0.55	Hydrophilic residue within 14-3-3 binding site on helix involved in RNA binding; predicted likely pathogenic
p.R1086C	severe	0.08	Close to FVYL pocket involved in P6.1 binding; Cys less hydrophilic; predicted likely tolerated.
p.R1086H	preserved	0.89	Close to FVYL pocket involved in P6.1 binding; His predicted tolerated.
p.V1090M	severe	<0.0	Surface residue; Met increases bulk; predicted tolerated but previously determined to be dysfunctional and disease-associated.
p.R1105W	intermediate	0.37	Very close to RNA backbone; Trp results in loss of positive charge; predicted likely pathogenic.
p.T1110M	intermediate	0.63	Poorly conserved surface residue at a distance from RNA; predicted tolerated.